Clinical, Cosmetic and Investigational Dermatology

Dovepress
Taylor & Francis Group

Open Access Full Text Article

ORIGINAL RESEARCH

Characterization of Ferroptosis-Associated Subtypes in Psoriasis and the Potential of CHAC1 as a Diagnostic Biomarker Based on Machine Learning

Junming Chen[1,2], Jiayi Zhan[1,2], Ying Zhou[1,2]

[1]Institute of Dermatology and Venereal Diseases, Department of Dermatology and Venereal Diseases, Affiliated Hospital of Guangdong Medical University, Zhanjiang, Guangdong, People's Republic of China; [2]The First Clinical College, Guangdong Medical University, Zhanjiang, Guangdong, People's Republic of China

Correspondence: Ying Zhou, Institute of Dermatology and Venereal Diseases, Department of Dermatology and Venereal Diseases, Affiliated Hospital of Guangdong Medical University, 57 Renmin Avenue South, Zhanjiang, Guangdong, 524002, People's Republic of China, Email zhouy10000@126.com; zhouy3183@gdmu.edu.cn

Purpose: Ferroptosis, a form of iron-dependent lipid peroxidation cell death. However, the mechanism of ferroptosis in psoriasis remains to be further investigated. Therefore, our research focuses on uncovering the role of ferroptosis in the pathogenesis of psoriasis and providing accurate biomarkers as therapeutic targets.

Patients and Methods: We merged differentially expressed genes (DEGs) from the gene expression omnibus (GEO) with ferroptosis-related genes from FerrDb database. Key genes were further identified using weighted gene co-expression network analysis (WGCNA) and machine learning. Additionally, we used non-negative matrix factorization (NMF) clustering to identify two ferroptosis molecular subgroups.

Results: CHAC1, PARP9 and LCN2 are identified as key ferroptosis-related genes in psoriasis. The psoriatic skin samples were divided into cluster 1 and cluster 2, with cluster 1 being the more severe subtype of psoriatic lesions. The expression of CHAC1 had the highest correlation with activated CD4 T cells, neutrophil, regulatory T cell (Tregs) and type 2 T helper cell (Th2), which were significantly enriched in cluster1.

Conclusion: In conclusion, the ferroptosis associated diagnostic gene CHAC1 exacerbates psoriasis by regulating activated CD4 T cells, neutrophil, Tregs and Th2, serving as a reliable biomarker to predict patient survival.

Keywords: molecular subgroup, bioinformatics analysis, ferroptosis-related genes, immune cell

Introduction

Psoriasis is a persistent systemic inflammatory skin disease characterized by abnormal proliferation and differentiation of keratinocytes caused by persistent inflammation.[1] Affecting 2% to 3% of the world's population, psoriasis appears as red patches with silvery scales and is associated with an increased risk of cardiovascular and other diseases.[2] Nonetheless, the pathogenesis remains largely unknown. Biological drugs have been at the forefront of clinical research over the past decade and are expected to improve disease remission rates and reduce the associated long-term risks.[3] Side effects, drug resistance, and other problems associated with biologics also limit their use.

Studies have indicated that ferroptosis is associated with sustained release of damage-associated molecular patterns (DAMPs) and cytokines that exacerbate the inflammatory response.[4,5] Ferroptosis has been shown to trigger and escalate inflammation,[6] and ferroptosis inhibitors exhibit anti-inflammatory properties in various disease models.[7] Recent findings demonstrate that ferroptosis-associated cell death is activated in psoriatic lesions, with similar ferroptotic trends observed in human primary keratinized cells treated with erastin and in IMQ (imiquimod) -induced psoriasis models. Overall, the

Received: 12 July 2025
Accepted: 15 November 2025
Published: 2 December 2025

targets, mechanisms, therapeutic agents, and clinical validation of studies to treat psoriasis by modulating ferroptosis pathways remain unclear and more evidence is needed.

A study reveals that glutathione (GSH) plasma levels and GSH peroxidase activity are markedly lower compared to the general populace in psoriasis patients.[8] CHAC1 emerges as a potential gene within the GSH metabolism signaling pathway, noted for its high catalytic efficiency and an upsurge in CHAC1 expression precipitates GSH depletion and disrupts cellular redox balance,[9] which indicates the potential role of CHAC1 in psoriasis. The upregulation of CHAC1 is widely accepted as an early ferroptotic marker. In the context of ferroptosis, CHAC1 degradation of GSH enhances susceptibility to ferroptosis under cystine starvation conditions.[10] miR-432-5p binds to the 3′UTR of the CHAC1 gene, and this suppression leads to the accumulation of GSH, which in turn activates GPX4 and prevents lipid peroxidation, thereby inhibiting ferroptosis.[11] In addition, a research uncovered PARP9 active involvement in psoriasis-related pathways, and substantial correlations with immune cells and oxidative stress were noted.[12] An important ferroptosis-regulating protein under physiological and inflammatory settings has been identified as LCN2.[13] According to earlier research, the main iron-regulatory functions of LCN2 during inflammation include iron scavenging, regulating the levels of cytoplasmic ferroptosis, reducing oxidative stress, and transporting iron between cells, tissues, and organs.[14,15] LCN2 has been implicated in psoriasis pathogenesis by modulating neutrophil activity and local skin inflammation via the SREBP2-NLRC4 axis.[16,17]

Therefore, it is crucial to understand the biological function of ferroptosis in the pathogenesis of psoriasis and to explore whether ferroptosis-related genes (CHAC1, LCN2 and PARP9) can be used as accurate biomarkers for psoriasis to provide effective therapeutic targets in biologics research.

GSE30999, training set of our research, contains a transcriptome of 85 paired skin lesion samples and non-lesion samples from a group of patients with moderate-to-severe generalized psoriasis who are not receiving active psoriasis treatment, providing the most comprehensive molecular definition of moderate-to-severe disease based on lesional skin. What's more, GSE13355 and GSE14905, which are from the same sequencing platform as the training set, also compare the molecular expression differences between skin lesion and NL samples. Including them as validation sets not only reduces cross-platform integration errors but also ensures disease-specific conclusions by using NL tissues as "health-like controls" to avoid potential confounders like age and environmental exposure between healthy donors and patients.

In this study, we use GSE30999 dataset to investigate the biomarkers and molecular mechanisms associated with psoriasis, focusing on the role of ferroptosis. We employed machine learning algorithms to identify core genes involved in ferroptosis and analyzed their expression patterns and regulatory mechanisms using non-negative matrix factorization (NMF) clustering and immune infiltration analysis. Our findings highlight the significance of ferroptosis in psoriasis, revealing two distinct clusters, screening for biomarkers (CHAC1, LCN2 and PARP9) related to ferroptosis. Additionally, we propose a relationship between CHAC1 expression and the activation of CD4 T cells, neutrophils, regulatory T cells (Tregs), and Th2 immune cells, which correlates with disease severity.

Methods

Data Download and Preprocessing

A concise flow chart can be seen in Supplementary Figure 1.

All data used in this study are freely available to the public. First, we downloaded the sample source from the Gene Expression Omnibus (GEO) (https://www.ncbi.nlm.nih.gov/geo/) database. The GSE30999 dataset includes 85 non-lesion (NL) and 85 psoriasis skin biopsies, the GSE13355 dataset consists of 58 psoriasis patients and 64 NL skin group, with a total of 58 psoriasis samples and 122 NL skin samples, and the GSE14905 dataset comprises skin biopsies from 21 normal healthy donors, 56 psoriasis skin biopsies from 28 psoriasis patients with matched diseased and non diseased tissues, and 5 samples from patients who only provided diseased skin biopsy. To explore differential methylation in psoriatic lesion epidermis, we selected the GSE103038 dataset, which contained 9 control samples and 3 experimental samples. It features exhaustive genome-wide DNA methylation analysis using reduced representation bisulfite sequencing, and compares lesional and non-lesional epidermis from psoriasis patients with epidermis from healthy controls, focusing on epigenetic modifications in skin unaffected by psoriasis. Due to its limited number of clinical samples, more

Table 1 Descriptive Statistics

GEO(ID)	Platform	Tissue (Homo Sapiens)	Samples (Number)		Attribute
			NL	Psoriasis	
GSE30999	GPL570	Skin	85	85	Training
GSE13355	GPL570	Skin	58	122	Validation
GSE14905	GPL570	Skin	49	33	Validation
GSE103038	GPL18460	Skin	9	3	Methylation

Notes: GPL570 (Affymetrix Human Genome U133 Plus 2.0 Array); GPL18460 (Illumina HiSeq 1500).

studies are needed for further validation in the future. The data information is shown in Table 1. Transform the "probe id" in the expression matrix into the "symbol" using the normalize Between Arrays function in the limma R package to normalize all gene expression profiles. We determine the expression level for several probes with the same gene symbol by averaging their values.

The world's first database devoted to ferroptosis regulators and ferroptosis illnesses is named FerrDb V2 (http://www.zhounan.org/ferrdb/). Seven hundred and twenty-eight ferroptosis-related genes were downloaded from FerrDb V2 database, including 369 Driver, 348 Suppressor and 11 Marker genes. There are 244 multi-annotation genes and 484 FRGs.

Weighted Gene Co-Expression Network Analysis

Weighted gene co-expression network analysis (WGCNA) identified gene modules using hierarchical clustering and designated them with colors. The dynamic tree cut method was applied to recognize distinct modules. During module selection, the adjacency matrix (a measure of topological similarity) was transformed into a topological overlap matrix (TOM), and modules were detected through clustering analysis. The association between module eigengene (ME, the first principal component of the module representing its overall expression level) and psoriasis was calculated via Pearson correlation analysis. Modules significantly associated with psoriasis were obtained. The co-expression module structure was visualized through a heatmap of topological overlaps in the gene network. Relationships among modules were summarized by hierarchical clustering trees of eigengene networks and corresponding eigengene heatmaps. The most crucial component of each module is its feature genes, which are estimated as synthetic genes that reflect the expression patterns of all the genes in a certain module.

Differential Expression Analysis

By comparing the expression values of samples from the normal and psoriasis group, differentially expressed genes (DEGs) were screened using the limma R package. The filtering criteria for this DEGs are as follows: absolute foldchange value >0.8 and P-value <0.05. Using ggplot2 R package to draw volcano map. Then, take the intersection of DEGs and FRGs to obtain the ferroptosis-related differential expressed genes.

Gene Function Enrichment Analysis

We used the "clusterProfiler" and "org.hs.egg.db" R packages to analyze biologically significant integrative functions and to annotate the human genome. Gene ontology (GO) includes biological process (BP), molecular function (MF) and cellular component (CC). Kyoto Encyclopedia of Genes and Genomes (KEGG) is a well known database preserving genomes and biological pathways.

Gene set enrichment analysis (GSEA) uses a predefined set of genes (usually the result of previous analyses or from functional annotations) to rank the genes based on the degree of differential expression in the two types of samples, and then tests whether that predefined set of genes is enriched at the top or the bottom of that ranked list. GSEA analysis was performed on the expression matrices of the psoriasis and control groups using the clusterProfiler R package. A non-parametric, unsupervised method called gene set variation analysis (GSVA) was used to determine the enrichment scores

for certain gene sets in each sample. To compare patients with psoriasis to controls, gene sets were downloaded and read using the msigdbr R package, and GSVA scores were calculated using the limma R package.

Protein–Protein Interaction Network Analysis

The protein–protein interactions (PPI) network was analyzed using the STRING database (https://string-db.org) and visualized using Cytoscape software. Genes without nodes were excluded. With the NetworkAnalyst online tool, we used TF and gene target data obtained from ENCODE ChIP-seq data to construct gene regulatory networks of gene-transcription factor (gene-TF) interaction networks. According to the BETA - Minus algorithm, the screening criteria were including peak intensity signal <500 and predicted regulatory potential score <1. Besides, NetworkAnalyst was used to construct protein–chemical interaction networks. Protein–chemical interactions were obtained from the Comparative Toxicogenomics Database, which contains chemical–gene interactions from the literature.

Identification of Hub Genes

In order to identify key biomarkers for predicting psoriasis lesions, we employed eight machine learning algorithms using Rstudio (version: 4.4.1), including gradient boosting decision tree (GBDT), randomForest (RF), recursive feature elimination (RFE), SVM-RFE, least absolute shrinkage and selection operator (LASSO), eXtreme gradient boosting (XGBoost), bootstrap aggregation (Bagging), and Boruta, respectively. The feature genes obtained from the various algorithms are intersected to obtain the key genes that are biologically important in psoriasis.

Each iteration of GBDT trains the next classifier based on the prediction error of the current model. The "randomForest" (Version: 4.6–14) and "caret" (version: 4.4.1) R packages are used to construct RF and SVM-RFE. RF, one of the most commonly used machine learning algorithms, utilizes multiple trees to train and predict samples, and ranks the most predictive variables. What's more, the "mlbench" (version: 4.1.3) and "caret" R packages are utilized for RFE analysis to find the best combination of variables by adding or removing specific variables. In addition, the purpose of utilizing the "glmnet" (version: 4.2.3) R package is to perform LASSO analysis using turn/penalty parameters and 10-fold cross-validation data. XGBoost, an optimized distributed gradient enhancement library, is an efficient implementation of machine learning algorithms in the gradient boosting framework. Bagging is an integrated learning algorithm that avoids overfitting by reducing the variance of the results. Boruta algorithm is a supervised classification feature selection method for identifying all the relevant features for a classification task.

Construction and Verification of Nomogram

Nomogram can be used to explore relationships and interactions between multiple variables as well as to assess the extent to which different variables influence an outcome. The "regplot" R package is used to generate nomogram describing key genes. Clinical calibration curves are used to compare actual and predicted incidence rates. Also, decision curve analysis (DCA) and clinical impact curves are plotted to analyze the clinical benefits of models.

Identification of Molecular Subtypes

NMF is a novel machine learning algorithm based on high-throughput data for identifying and clustering different molecular functional patterns. In this study, the expression profiles of FRDEGs in psoriasis samples were used as input data, and the psoriasis lesions were clustered using the "NMF" R package according to the "brunet" selection criterion with 50 iterations, and the optimal clusters were selected based on the cophenetic selection. The optimal number of clusters selected by cophenetic, k=2, was used to further characterize different ferroptosis-associated psoriasis subtypes. Principal component analysis downscaling differentiated cluster1 and cluster2.

Immune Infiltration Analysis

In this study, we used the CIBERSORT technique to calculate the level of immune cell infiltration in the normal individuals and psoriasis patients. We use 22 immune cells as the default feature gene file group. Besides, the gene profiles expressed by immune cell populations were quantified using the single sample gene set enrichment analysis (ssGSEA) function. Differences in immune cell infiltration between psoriasis patients and healthy controls were calculated using $P < 0.05$ as

the criterion for significance. Correlations between the levels of immune cell infiltration of different types of immune cells were calculated using Pearson's correlation based on the ssGSEA score of immune cell type.

Methylation Analysis

The 450 K array methylation level profiles of nine NL skin tissues, and three psoriatic skin tissues from the GSE103038 dataset were selected. The methylation profiles of 9 NL skin group samples and 3 psoriasis samples were analyzed by differential methylation probes (DMPs) using the "ChAMP" R package. Meanwhile, the methylation expression levels of CHAC1, LCN2 and PARP9 were visualized using the "ggplot2" R package.

Statistical Analysis

Statistical analysis was performed using R software (version 4.2.1). Spearman correlation was employed to assess the correlation between two parameters, and Wilcoxon test was conducted to compare differences between two groups. A significance level of $P < 0.05$ was considered statistically significant.

Results

Weighted Gene Co-Expression Network Analysis

To identify outlier sample values for further analysis, we conducted sample cluster analysis (Figure 1A). A soft threshold of power = 7 ensures that the network is scale-free (Figure 1B). To investigate the relationship between ME genes and psoriasis, a total of 12 modules were generated, and the clustering tree diagram is shown in Figure 1C. Calculate and plot the correlation between each module and psoriasis (Figure 1D). The module with the highest correlation with psoriasis is turquoise with 1863 genes, ($r=-0.91$, P=2e-66). The significance of turquoise color module and psoriasis genes was cor=0.97, P<1e-200 (Figure 1E).

Identification of Differentially Expressed Genes

A total of 20857 genes were identified in GSE30999, and 2655 DEGs were generated based on gene differential analysis. Among them, 1358 were low expression and 1297 were high expression, as shown in Supplementary Table 1. Visualize the results using a volcano map (Figure 2A) and a heatmap (Figure 2B). Figure 2C shows the association of genes. In addition, FerrDb's 484 FRGs intersected GeneCards with 2655 DEGs, resulting in 61 FRDEGs. Then, these FRDEGs were hybridized with the module genes using WGCNA to obtain 28 genes, referred to as "intersect genes". The box plot (Figure 2D) shows the expression of 28 intersect genes. The PCA images of the normal group and psoriasis group samples are shown in Figure 2E. In addition, a Venn diagram (Figure 2F) was drawn to illustrate the intersection of genes.

Differentially Expressed Genes Enrichment Analysis

To further explore the potential mechanism of gene regulation in psoriasis pathogenesis, we performed GO and KEGG enrichment analysis. Among the MF categories, the most prominent were "actin binding", "iron ion binding" and "peptidase regulator activity". Important pathways of CC are focused on "cell cortex", "cornified envelope" and "cortical cytoskeleton". The major pathways of BP focus on skin development, such as "epidermis development" and "fatty acid metabolic process" (Figure 3A), while KEGG's prominent pathway is "insulin resistance" (Figure 3B). The GSEA results (Figure 3C) focused on the pathways related to immune response such as "innate immune response", "defense response to other organism" and "immune response". The GSVA results showed that the most significant up-regulated pathway was "abnormality of nail color", while the most significant down-regulated pathway was "nephric duct development" (Figure 3D).

Machine Learning Screening of Key Genes

Eight machine learning methods, including GBDT, RF, RFE, SVM-RFE, LASSO, XGBoost, Bagging, and Boruta, were used on the GSE30999 dataset to examine 28 intersect genes.

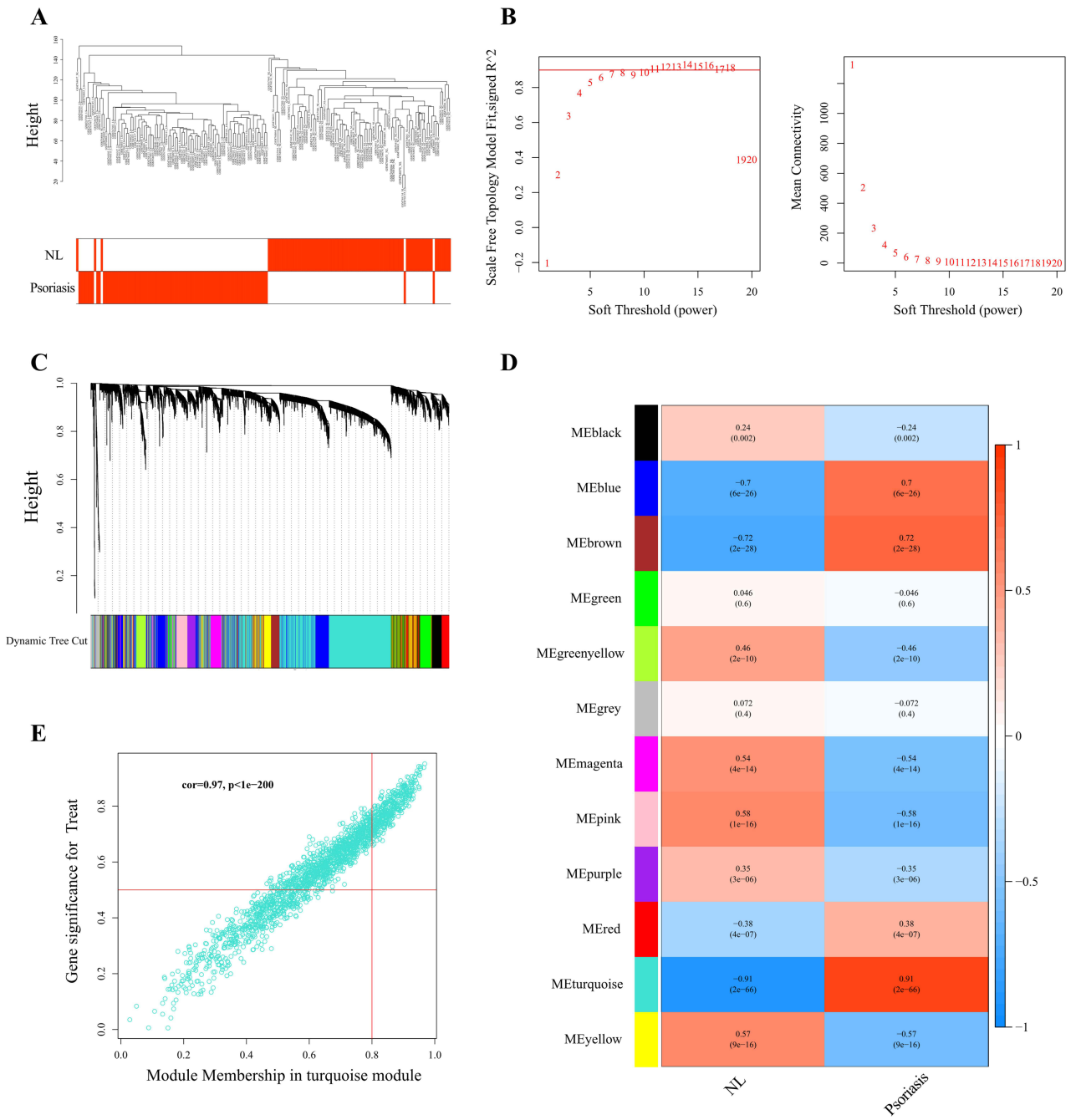

Figure 1 Construction of co-expression network modules. (**A**) Sample dendrogram and trait heatmap with tree leaves corresponding to individual samples. (**B**) Analysis under various soft-threshold powers. (**C**) Clustering dendrogram of various similarity genes using chosen module colors and topological overlap. (**D**) Associating modules with traits. Each row corresponds to a module, and each column corresponds to a feature. (**E**) Relationship between module membership and gene significance in turquoise module.

We used LASSO logistic regression to select 11 predictor genes from statistically significant univariate and adjusted the penalty parameters by 10-fold cross-validation (Figure 4A and B). Next, RF was used to screen 10 genes based on feature selection, number of classification trees, and error rate pairing (Figure 4C). The SVM-RFE algorithm similarly detected 10 genes as the best characterized genes (Figure 4D and E). In RFE feature selection, 9 genes were screened based on RMSE to determine the optimal model (Figure 4F). A total of 23 genes were screened based on Boruta's z-score variation (Figure 4G and H). Finally, we plotted the intersection of the marker genes obtained by the eight algorithms (Figure 4I and Supplementary Table 2) and identified CHAC1, LCN2 and PARP9 as key genes for further analysis.

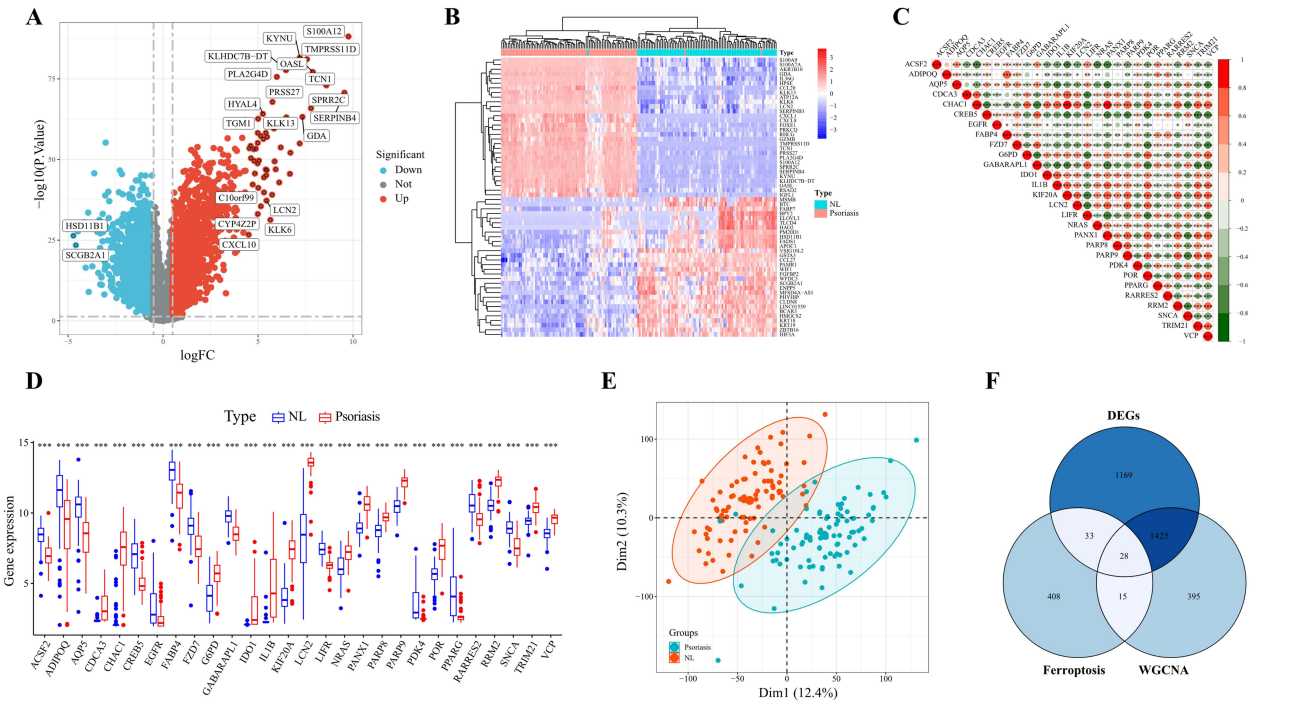

Figure 2 Screening of differentially expressed genes in psoriasis. (**A**) Differential analysis of volcano plot between the NL skin group and the psoriasis group. The red dots indicate strong expression, while the blue dots indicate low expression. (**B**) Heat map for difference analysis between the NL skin group and the psoriasis group. (**C**) Correlation map between genes and gene expression. (**D**) Differential box plot of 28 intersect genes. (**E**) PCA images of the normal group and psoriasis group. (**F**) Venn diagram of cross genes in DEGs, FRGs, and WGCNA module genes. *P < 0.05, **p < 0.01, ***p < 0.001.

Meanwhile, we mapped the 3 key genes into a nomogram (Figure 5A). The stability and diagnostic performance of the nomogram were demonstrated by further evaluation through clinical calibration and DCA (Figure 5B and C), suggesting that the model consisting of three genes, CHAC1, LCN2 and PARP9, is clinically effective in the diagnosis of psoriasis. Finally, we can see that the gene model composed of CHAC1, PARP9 and LCN2 has a better predictive ability in the clinic through the clinical impact curve (Figure 5D).

Protein–Protein Interactions and Related Functional Network Construction

We performed a PPI network analysis of FRDEGs, using the Cytoscape tool to measure and visualize the genes in the network (Supplementary Figure 2A). This generated a network containing 51 nodes and 276 edges. Also, we generated a network containing 24 nodes and 50 edges using 28 intersect genes (Supplementary Figure 2B). Gene-TF networks were created to explore the potential biological roles of hub genes in psoriasis (Supplementary Figure 2C). To further understand the potential therapeutic effects, we used online network analysis and constructed mRNA-chemistry networks (Supplementary Figure 2D).

Classification of Molecular Subtypes

The expression matrix of 61 FRDEGs was used as input data for NMF analysis (Supplementary Figure 3A and B). PCA clearly distinguished cluster1 and cluster2 (Supplementary Figure 3C). Differential analysis of FRDEGs was performed for cluster1 and cluster2, with cluster1 being the experimental group with 49 psoriasis samples and cluster 2 being the NL skin group with 36 psoriasis samples. Using |log foldchange value| >0.5 and P-value <0.05 as the threshold, there were 22 down-regulated and 14 up-regulated genes, totaling 36 degs. Next, we demonstrated the distribution of degs between the two subtypes by bar graph, volcano plot and heat map (Supplementary Figure 3D–F).

There is literature on the characterisation of degs in psoriasis. FADS1 and FADS2, as genes encoding key proteins for lipid metabolism and transport, are highly expressed in both atopic dermatitis and psoriatic sebaceous glands, and are essential for an effective acute inflammatory response and for maintaining epithelial homeostasis;[18] IDO1 acts as an

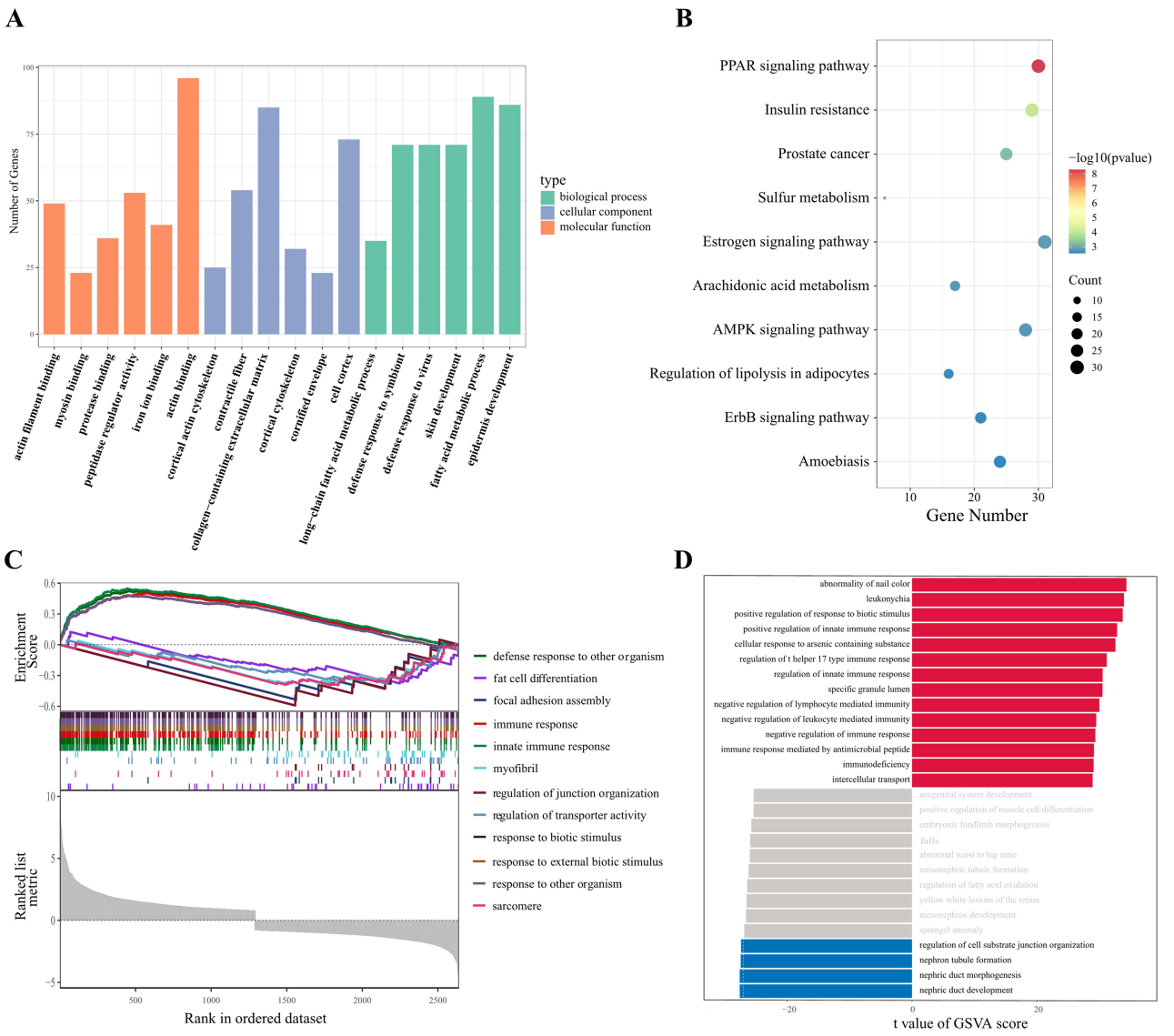

Figure 3 Biological function analysis of differentially expressed genes. (**A**) GO enrichment was detected by BP, CC and MF, showed in different colors. (**B**) KEGG enrichment analysis. (**C**) The 12 most important pathways in GSEA. The middle portion of the region shows where each gene in the gene set appears in the sorted list of genes. (**D**) Bar graph of GSVA showing significant and non-significant pathways. Gray modules are non-significant pathways, and red and blue modules are high and low expression significant pathways, respectively.

important immunomodulatory site involved in peripheral immune tolerance, and exerts a protective role in psoriasis by inducing regulatory T-cells;[19] Haem oxygenase-1 (HMOX1) offers protection against programmed cell death and induction of HMOX1 may be a promising approach for the treatment of psoriasis;[20] MGST1-related pathways include innate immune disorders, are associated with prostaglandin E and leukotriene synthesis, and are under-expressed in psoriatic lesion skin;[21] MUC1 plays a role in the formation of protective mucus barriers on epithelial surface, with higher expression in involved psoriatic lesions than in uninvolved and normal skin, especially in the early stages;[22] and NR1D2 expression is up-regulated in blood samples from psoriasis patients. The value of NR1D2 as a potential psoriasis biomarker was highlighted by predicting disease stage with 86% accuracy by using expression ratios of three gene pairs including NR1D2 and COX2.[23] Next, differences in the expression of the immune checkpoint IDO1 were demonstrated with violin plot (Supplementary Figure 3G).

Figure 6A shows the results of GO and KEGG analyses of degs between subtypes. The most significantly enriched pathway in the KEGG results was “Ferroptosis”. GSEA analysis showed that the degs were mainly enriched in the

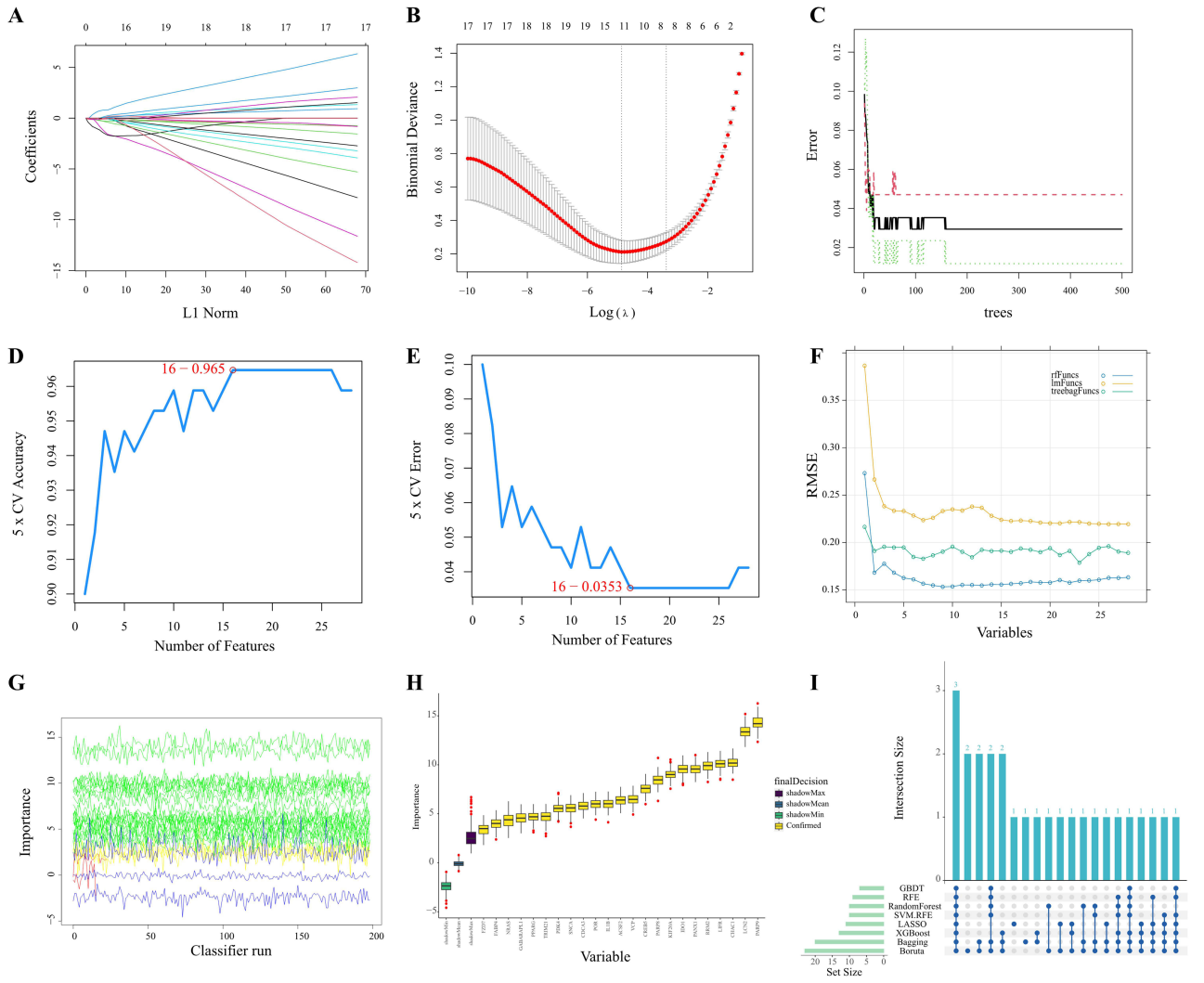

Figure 4 Identification of disease signature genes. (**A**) LASSO path parameters and corresponding selected features for each fold. (**B**) LASSO coefficient curves for the 28 intersecting genes. The two dashed lines indicate two specific values of λ, one is lambda. minimum and the other is. 1se, and the lambda between these two values is considered reasonable. (**C**) RF error rate versus classification tree count. (**D**) Predicted true value change curve. The fig.16–0.965 means that there are 16 features with an accuracy of 0.965. (**E**) Predicted error value change curve. 16–0.0353 is an indication that there are 16 features with an error rate of 0.0353. (**F**) Screening the best models for RFE using RMSE as a criterion. (**G**) Plot of z-score changes. Green, red, blue, and yellow show important, unimportant, shadow, and tentative variables, respectively. (**H**) Box plot showing the 23 characterized genes screened by Boruta's algorithm and sorted. (**I**) Intersection of eight machine learning algorithms.

"apoptotic process", "programmed cell death" and "cell death" pathways (Figure 6B), and all of them were characterized by "CHAC1", "IL1B", "IDO1", "POR", ATG7 '. Figure 6C shows the significant differential pathways analyzed by GSVA by heatmap, which shows that cluster2 is significantly enriched in 'negative regulation of epithelial cell proliferation','positive regulation of intrinsic apoptotic signaling pathway and "positive regulation of apoptotic signaling pathway". According to the characterization of the degs and the results of GSVA, we hypothesize that cluster1 is a subtype with severe psoriasis lesions, whereas cluster2 belongs to the subtype with mild psoriasis lesions. CHAC1 regulates the cell death process in cluster 1 patients, thereby exacerbating the pathogenesis of psoriasis.

Immune Cell Infiltration of Ferroptosis-Related Molecular Subtypes

As shown by the heatmap, activated CD4 T cells, neutrophil, regulatory T cells (Tregs) and type 2 T helper cells (Th2) were predominantly upregulated mainly in cluster 1. (Figure 6D). In addition, there was a significant positive correlation between immune cells (Figure 6E). Notably, activated CD4 T cell had a highly significant positive correlation with neutrophil, Tregs and Th2 ($p<0.001$). Next, we investigated the relationship of key genes CHAC1, LCN2 and PARP9

https://doi.org/10.2147/CCID.S553367

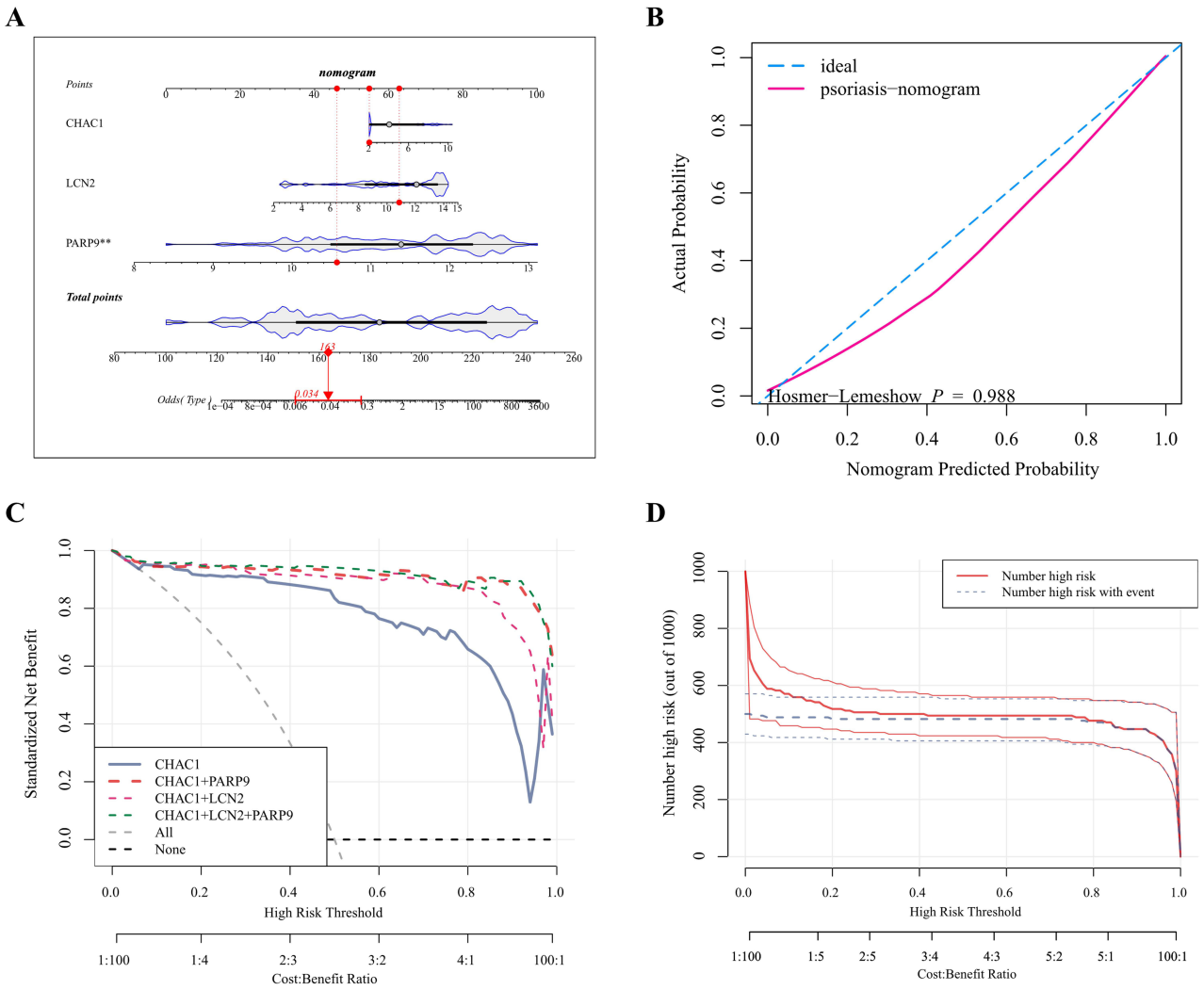

Figure 5 Validation of diagnostic efficacy of key genes. (**A**) Nomogram showing predicted risk based on CHAC1, LCN2 and PARP9. (**B**) The calibration curve demonstrates nomogram predictive performance by the extent to which the calibration curve deviates from the diagonal (ideal case). (**C**) DCA quantifies net benefit under different threshold probabilities. (**D**) Clinical impact curve.

with immune cells separately (Figure 6F). Interestingly, CHAC1 was not only significantly positively correlated with most of the immune cells but was also most was associated with the 4 immune cells mentioned above.

Analysis of the Role of CHAC1 in Regulating Immune Cells in Molecular Subtypes

The median value of CHAC1 (7.572235) was used to classify psoriasis samples into high- and low-expression subgroups. Differences in the expression of different immune cells in two groups were assessed by ssGSEA (Figure 7A). In the CHAC1 high expression subgroup, the infiltration level of activated CD4 T cells with neutrophil, Tregs and Th2 were significantly increased ($p<0.001$). Next, the relationship between CHAC1 and above 4 immune cell populations in psoriasis patients was demonstrated (Figure 7B–F). The results showed that the expression level of CHAC1 was positively correlated with all 4 psoriasis-associated immune cells mentioned.

The Expression Level of CHAC1 and Its Predictive Role in Diagnosis

In the training set GSE30999, the expression level of CHAC1 in psoriasis patients was significantly higher than that in the NL skin group (Supplementary Figure 4A). The validation sets GSE13355 (Supplementary Figure 4C) and GSE14905 (Supplementary Figure 4E) confirm this. The analysis results of receiver operating characteristic (ROC) curves showed that

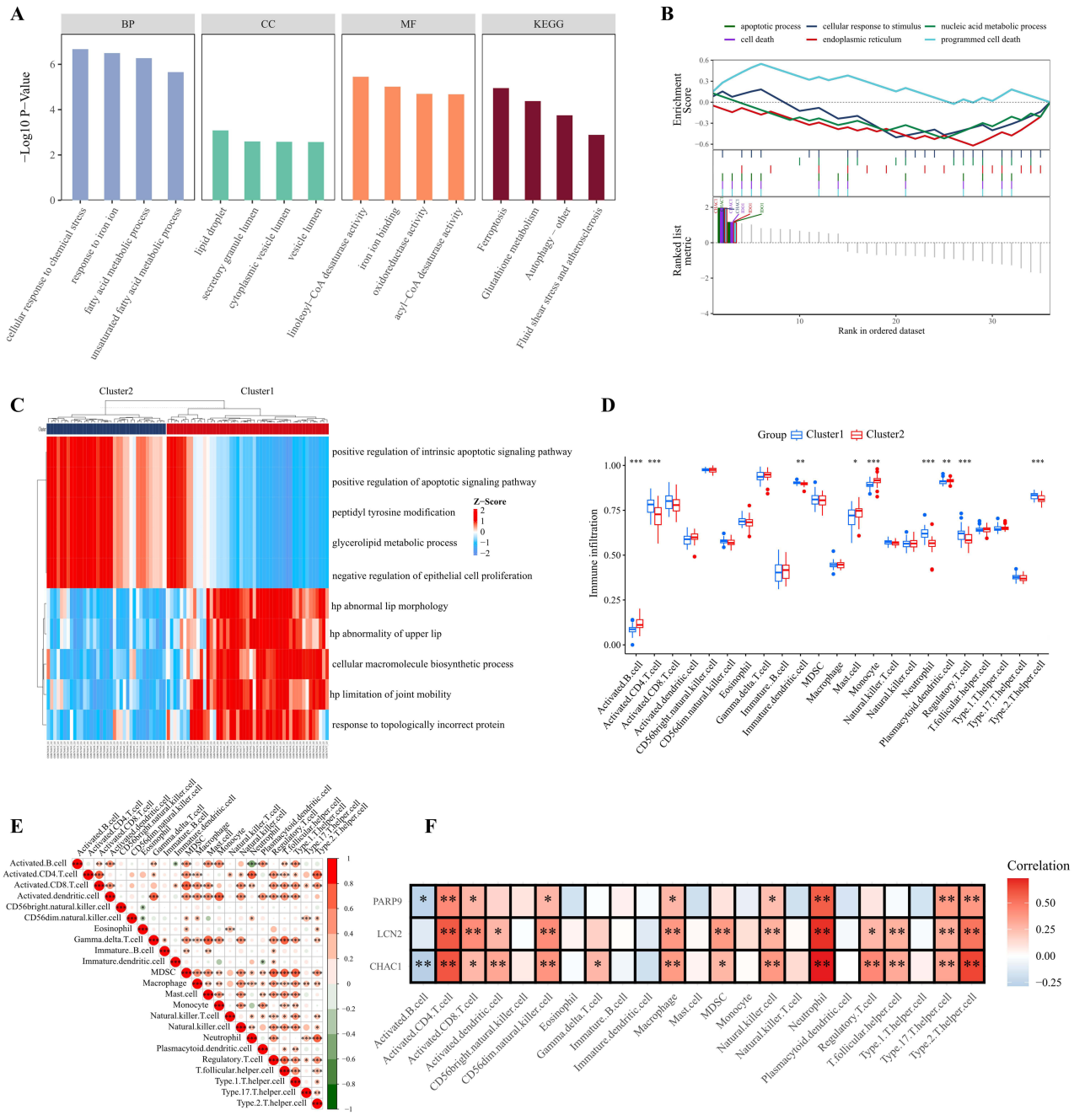

Figure 6 Identification of two ferroptosis molecular subtypes in psoriasis. (**A**) Functional annotation of 61 FRDEGs using GO enrichment analysis. (**B**) GSEA analysis reveals the six most significantly enriched pathways. (**C**) GSVA analysis showed the 10 most significantly enriched pathways. (**D**) Differential expression of immune cells in ferroptosis molecular subtypes in psoriasis. (**E**) Bubble diagram showing a positive correlation between most immune cells. (**F**) Relationship of CHAC1, LCN2 and PARP9 with immune cells. *P < 0.05, **P < 0.01, ***P < 0.001.

CHAC1 can distinguish between patients and healthy samples. In GSE30999, the area under the curve (AUC) value was 0.968 (Supplementary Figure 4B), indicating its high specificity and sensitivity in diagnosing psoriasis. In the validation set, the AUC values of the ROC curves for GSE13355 (Supplementary Figure 4D) and GSE14905 (Supplementary Figure 4F) were 0.987 and 0.917, respectively, indicating that CHAC1 is a reliable tool for evaluating disease progression.

https://doi.org/10.2147/CCID.S553367

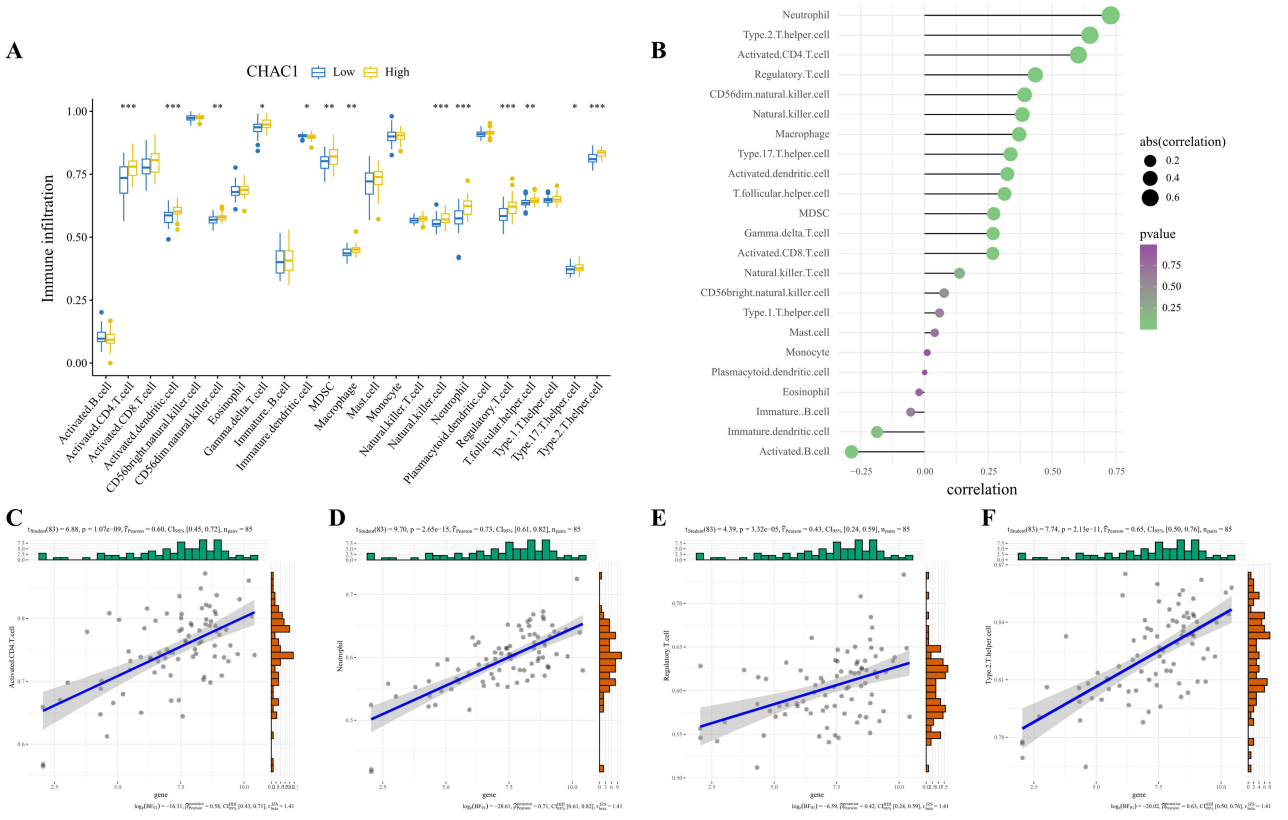

Figure 7 Immune-related cell landscape analysis for molecular subtypes of ferroptosis. (**A**) The different expression levels of immune cells in CHAC1 high and low expression groups. (**B**) CHAC1 immune cell-associated map under ssGSEA algorithm. (**C**–**F**) Correlation plots of CHAC1 expression levels with Activated CD4 T cell, neutrophil, Tregs and Th2 under ssGSEA algorithm, respectively.

Immune Infiltration of CHAC1

To further confirm the correlation between CHAC1 expression and immune cells, CIBERSORT algorithm was used to analyze the infiltration ratio of immune cells. As shown in Figure 8A, calculate the content of 22 types of cells in each sample using CIBERSORT. Correlation heatmap of the 22 immune cell types was also generated (Figure 8B). As shown in the violin diagram (Figure 8C), there are 4 types of cells with low expression and 9 types of cells with high expression in the disease group. By inputting CHAC1 and analyzing the relationship between gene expression and cell expression, 14 cells found a correlation between expression and CHAC1 expression. Among them, 9 cell expressions were positively correlated with CHAC1, and 5 were negatively correlated (Figure 8D). These results support that the level of CHAC1 may affect the activity of immune cells.

Methylation Biomarkers in Psoriasis

We examined GSE73894 to identify key psoriasis genes that may be modified by methylation. We generated a heat map of methylation levels based on the distribution and expression of DMPs on 22 autosomal chromosome and X and Y sex chromosomes and their chromosome arms, which showed significant differences in methylation expression between the psoriasis group and the NL skin group (Figure 9A). In addition, we investigated the location and distribution of DMPs in relation to high and low methylation levels (Figure 9B). Differences in gene methylation of CHAC1, LCN2 and PARP9 genes in NL skin group and psoriasis group were demonstrated by violin plots (Figure 9C–E).

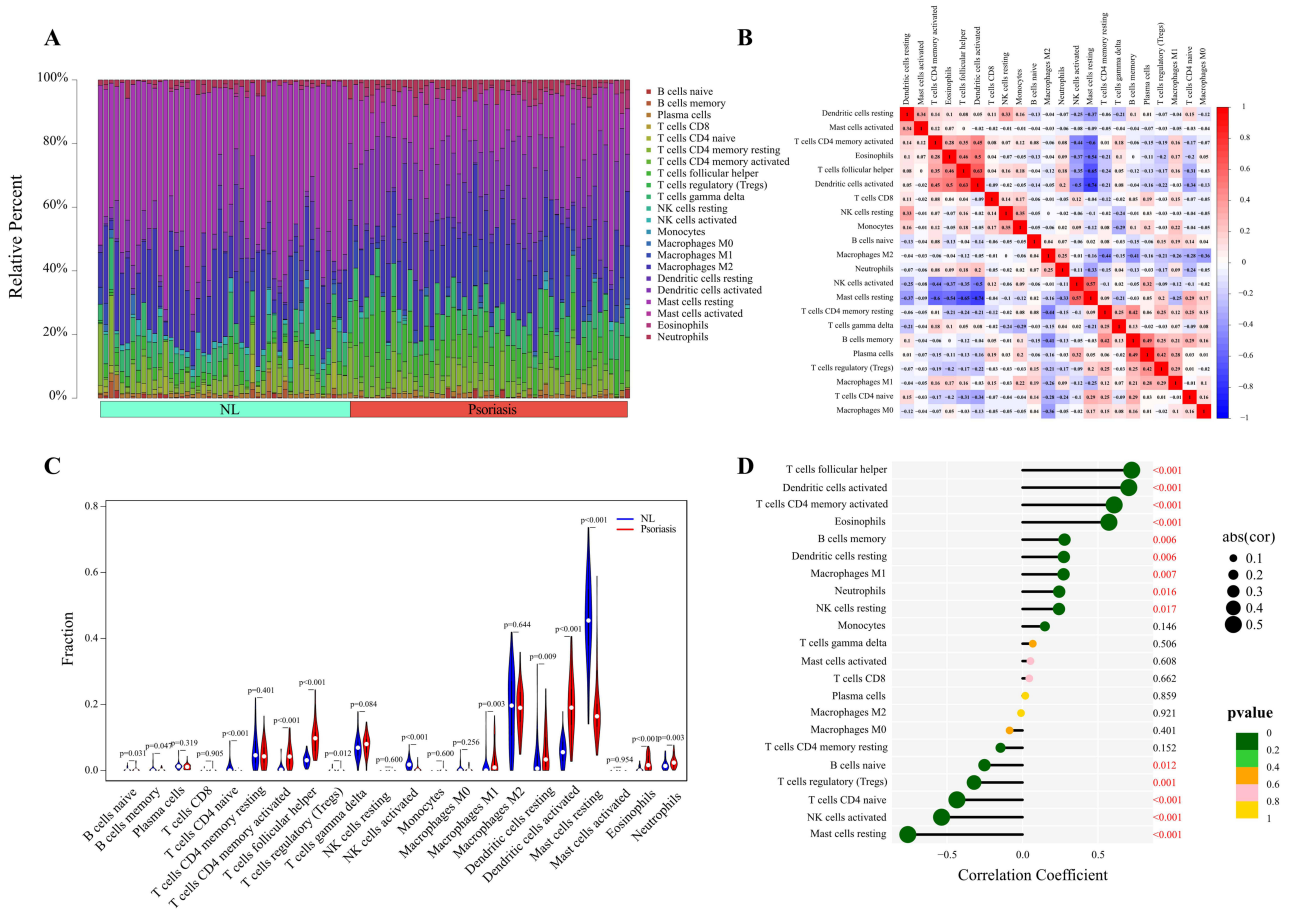

Figure 8 Evaluation and correlation analysis of immune cell infiltration in the GSE30999. (**A**) The bar chart displays the relative percentage of 22 immune cells in each sample. (**B**) Correlation analysis between immune cells. R value<0 indicates negative correlation, while R value>0 indicates positive correlation. (**C**) Violin plot of differential infiltration of all 22 immune cells. (**D**) Correlation analysis between CHAC1 and immune cells.

Discussion

Psoriasis, a pervasive and troublesome dermatological affliction, has garnered substantial focus from both clinicians and researchers. Characterized as a persistent immune-mediated condition, it predominantly impacts the skin and joints, often inducing psychological distress like anxiety.[24,25] Globally, psoriasis affects between 0.9% and 8.5% of adults and 0% to 2.1% of children.[26] Despite the extensive research into the disease's pathogenic mechanisms and the development of novel therapeutic approaches, recurrence remains alarmingly common, underscoring the pressing need for innovative, effective, and safe treatments.[27]

Ferroptosis has recently emerged as a groundbreaking mechanism of programmed cell death, showing a significant connection to various human ailments.[28,29] A study detected a concurrent elevation of lipid ROS and divalent iron in the psoriatic epidermis, a finding corroborated by transmission electron microscopy, which confirmed ferroptosis activation in both patient and mouse models of psoriasis.[30] Along with the elevation of PTGS2 mRNA, a established ferroptosis biomarker,[31] in psoriatic lesions, ferroptosis is putatively activated and contributes to inflammation. This occurs through the action of PTGS2-encoded COX-2,[32] which generates inflammatory mediators from arachidonic acid, and through the sensitization of Th22/Th17-type cytokines,[31] highlighting a pathogenic role for ferroptosis in psoriasis aggravation. The intricate interplay between ferroptosis and inflammation in psoriatic lesions suggests that targeting ferroptosis might offer a promising therapeutic avenue for psoriasis, warranting deeper exploration.[33] Hence, deciphering molecular patterns and pinpointing diagnostic biomarkers related to ferroptosis are crucial for managing psoriasis' onset and progression. In addition, keratinocytes exhibit aberrant proliferation and significant inhibition of apoptosis, and inhibition of apoptosis is

https://doi.org/10.2147/CCID.S553367

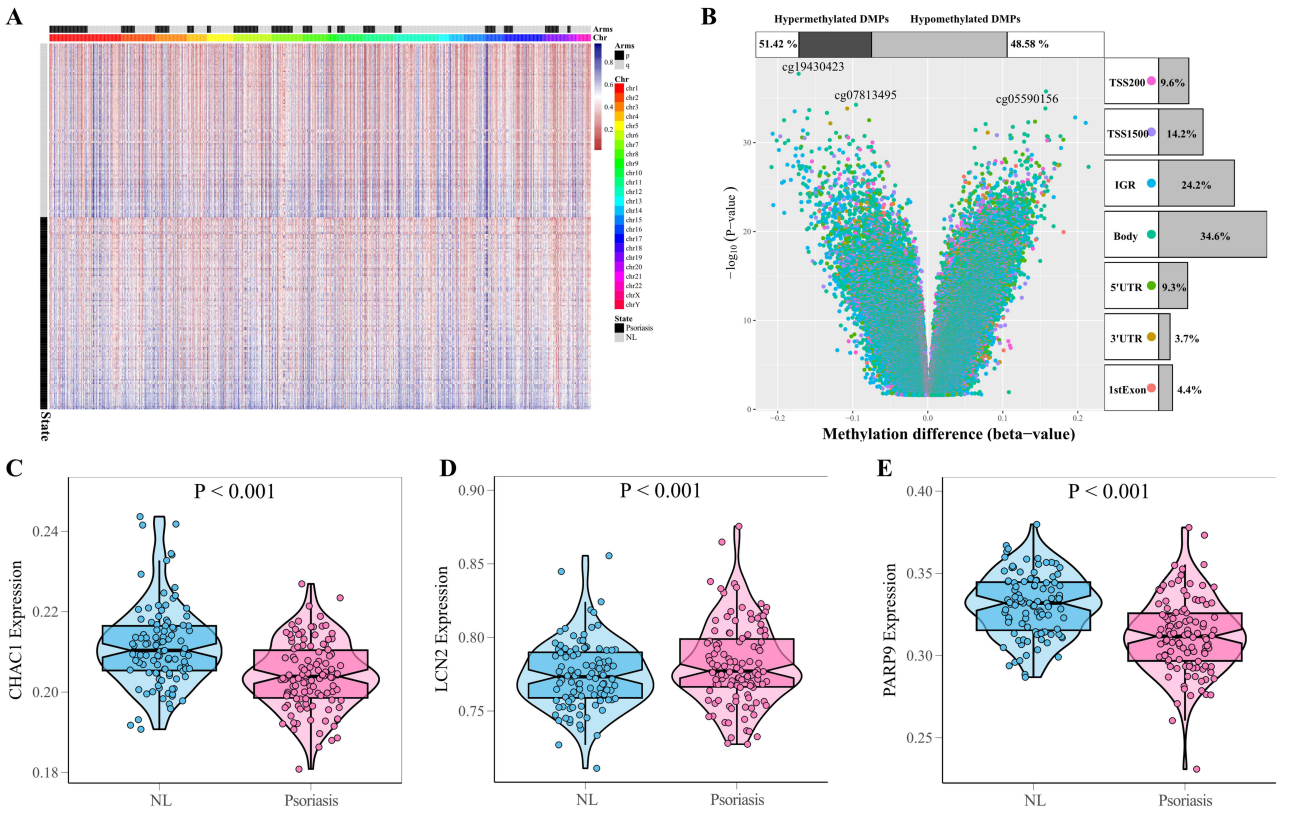

Figure 9 Identification of methylation levels of key genes. (**A**) Heat map of methylated probes between psoriasis group samples (n = 3) and NL skin group samples (n = 9). Probes (columns) are categorized by chromosomal location. (**B**) Differences in the distribution of DMPs between the psoriasis group and the normal group. (**C**–**E**) Violin plots showing the difference in methylation levels of CHAC1, LCN2 and PARP9 between the psoriasis group and the NL skin group.

associated with an imbalance in epidermal homeostasis and contributes to psoriatic hyperplasia.[34] The inflammatory microenvironment induced by ferroptosis (such as DAMPs release mentioned earlier) may inhibit apoptosis by activating BCL-2 family proteins, forming a positive feedback loop that promotes proliferation. Notably, ROS may co-exacerbate aberrant keratinocyte differentiation through dual regulation of ferroptosis and pyroptosis to form a cascade response (eg, through activation of NLRP3 inflammatory vesicles). Pyroptosis has been shown to correlate strongly with abnormal keratinocyte keratinization in vitro,[35] and ROS induce not only ferroptosis, but also pyroptosis.[36]

Our studies were conducted through a combination of transcriptomics (screening for differential gene function and enrichment analysis of pathways), proteomics (protein–protein interaction network construction and hub protein identification), and epigenetic analysis (genome-wide DNA methylation profiling and differentially methylated region identification). GO and KEGG analyses of DEGs revealed prominent pathways in MF, CC, and BP as “actin binding”, “cell cortex”, and “skin epidermal development”, respectively. KEGG analysis highlighted insulin resistance as a crucial pathway associated with psoriasis. Interleukin-2 inducible T-cell kinase (ITK) plays a significant role in Th2 cell-mediated autoimmune and allergic conditions like psoriasis by promoting T cell responses through actin binding.[37] What’s more, the cell cortex, referred to the actin cytoskeleton’s plasma membrane-associated segment, is crucial.[38,39] Psoriatic skin epidermal tissues show an increase in channel cells with heightened gene expression of psoriasis-associated keratins KRT6A and KRT16, and the risk gene GJB6.[40] This upregulation in inflamed skin can partly be attributed to the elevated presence of channel cells in normal skin.[41] The role of channel cell expansion in psoriasis or epidermal inflammation remains under investigation. Additionally, psoriasis is intimately linked with metabolic syndrome (MetS) features, such as type 2 diabetes and cardiovascular disease, with insulin resistance being a major risk factor.[42] GSEA results emphasize that DEGs predominantly influence immune-related pathways like the “innate immune response” and “defense against other organisms”, reinforcing the immune response’s critical role in psoriasis.

Our research pioneers the use of eight machine learning algorithms—GBDT, RF, RFE, SVM-RFE, LASSO, XGBoost, Bagging, and Boruta—to identify distinctive biomarkers linked to ferroptosis in psoriasis, revealing CHAC1 (ChaC Glutathione Specific Gamma-Glutamylcyclotransferase 1), PARP9 (Poly(ADP-Ribose) Polymerase Family Member 9), and LCN2 (Lipocalin 2) as stable biomarkers. Moreover, nomogram plot and analyses of clinical calibration and decision curves underscore the robustness and predictive prowess of the CHAC1, PARP9, and LCN2 gene model in clinical decision-making for psoriasis, demonstrating superior predictive capability when combining multiple biomarkers over a singular one. Endoplasmic reticulum (ER)-induced CHAC1 expression depletes GSH, compromises GPX4 function, and promotes ferroptotic cell death. It can also induce ferroptosis through mechanisms that are independent of ER stress. CHAC1 can induce ferroptosis independently of ER stress, primarily by depleting GSH and influence the expression of proferroptotic genes, enhancing lipid metabolism and iron uptake/storage, which collectively drive ferroptosis.[43] PARP9, which is implicated in the development of human and murine atherosclerotic plaques, may mechanistically link psoriasis to atherosclerosis through immune-mediated pathways.[44] A experimental study proposed that the LCN2-TWEAK-Fn14 loop plays a critical role in the interactions among keratinocytes, neutrophils, and macrophages.[45]

Enrichment analyses of the differential genes of cluster 1 and cluster 2 revealed that ferroptosis was the most significant result of KEGG enrichment. GSEA analysis reveals the six most significantly enriched pathways, including the "apoptotic process", "programmed cell death" and "cell-death" pathways. GSVA of these genes in NMF typing revealed that cluster2's significant differential pathways focused on "negative regulation of epithelial cell proliferation", "positive regulation of apoptosis intrinsic signalling pathway", and "positive regulation of apoptosis signalling pathway". Based on the degs characteristics and GSVA results in various clusters, cluster1 is proposed as a more severe psoriasis subtype with a poorer prognosis, while cluster2 represents a milder subtype with a more favorable prognosis due to metabolic pathway regulation. Ferroptosis-associated CHAC1 regulates the cell death process in cluster 1 patients, thereby exacerbating psoriasis severity.

To unravel the complexities of immune and metabolic landscapes associated with ferroptosis molecular subtypes in severe psoriasis and their implications for early intervention, we conducted a comprehensive immune infiltration analysis of cluster 1 and cluster 2 using ssGSEA. Our analysis revealed that activated CD4 T cells, neutrophils, Tregs, and Th2 were significantly upregulated in cluster 1, demonstrating a noteworthy positive correlation among these immune cells. This suggests that variations in immune infiltration across different ferroptosis subtypes are crucial to psoriasis pathogenesis. Intriguingly, CHAC1 exhibited the highest correlation with these 4 immune cell types. Spontaneous apoptosis of neutrophils plays a key role in maintaining immune homeostasis and resolving inflammation. Glutathione levels were reduced in apoptotic neutrophils. Intracellular GSH depletion during apoptosis may promote caspase-3 shearing through activation of the JNK pathway, whereas exogenous GSH inhibits this process by maintaining a reduced state. Exogenous glutathione and LPS treatment delayed neutrophil apoptosis and decreased levels of the pro-apoptotic protein caspase-3.[46] Immune infiltration analysis showed that CHAC1 expression showed a positive correlation with neutrophils. CHAC1-mediated GSH depletion may affect neutrophils through a dual mechanism: both by enhancing pro-inflammatory factor release (eg, IL-1β) through ferroptosis and by slowing apoptosis through decreased caspase-3 activity, creating a positive feedback loop of sustained inflammation.

By stratifying psoriasis samples into high and low CHAC1 expression subgroups based on median values and assessing immune cell expression differences via ssGSEA, we found a strong positive correlation between CHAC1 gene expression and the 4 aforementioned psoriasis-associated immune cells (activated CD4 T cells, neutrophils, Tregs, and Th2). T cells are essential for the initiation and maintenance of keratinocyte proliferation in psoriasis.[47] The onset of psoriasis appears to be linked to the influx of activated CD4 T cells,[48] which are prominent in the dermal skin of psoriasis patients.[49] Type 1 T helper cells (Th1), a crucial subset of activated CD4 T cells, amplify immune responses through interferon-g (IFN-g) and Tumor Necrosis Factor-α (TNF-α), pivotal in psoriasis development.[50,51] Neutrophil-rich munro'smicroabscess remain a key histopathological feature of psoriasis.[52] Elevated neutrophil-to-lymphocyte ratios (NLR) in psoriasis patients have been noted.[53,54] NLR levels decrease post-treatment, highlighting their role in disease progression.[55] Understanding neutrophil roles has driven the development of therapies aimed at mitigating their overstimulation in psoriasis.[56] Tregs often exhibit dysfunctional control over T-cell responses and proliferation in psoriasis patients.[57,58] Th17 cells, a subset of

CD4+ T cells, are highly active and infiltrate psoriasis lesions, indicating their significant role in disease pathogenesis. An imbalance between Th17 and Treg ratios, with impaired Treg suppression, represents a critical pathological shift in psoriasis.[59,60] While the precise role of Th2 cells in psoriasis remains obscure, we posit that Th2 cells might hold significant potential for research into psoriasis treatment. Key regulatory genes and immune cells involved in the pathogenesis of psoriasis have been the subject of ongoing research into therapeutic targets. Importantly, there has been no previous study investigating the interaction between CHAC1 and the 4 key immune cell types mentioned above in the context of psoriasis. Thus, our research pioneers a hypothesis that the ferroptosis associated diagnostic gene CHAC1 influences activated CD4 T cells, neutrophils, Tregs, and Th2 immune cells involved in immune infiltration, and enhances cellular ferroptosis response through NMF clustering and typing, thereby exacerbating the progression of psoriasis in patients. However, due to the lack of clinical data in GSE30999, to demonstrate the stability of the identified subtypes or biomarkers across different clinical subtypes, more experimental study needs to be carried forward.

The regulatory mechanisms of necroptosis and ferroptosis are highly interconnected. For instance, compared with healthy uninvolved skin, psoriasis lesions exhibit a significant decrease in GPX4. GPX4 overexpression reduces mitochondrial ROS and concurrently prevents both ferroptosis and necroptosis.[61] A study found the overexpression of CHAC1 elevates ROS, inducing mitochondrial dysfunction. The resulting amplification of oxidative stress ultimately culminates in cell death via both ferroptosis and necroptosis pathways. Previous literature has shown that the significant reduction of GPX4 in psoriatic lesions may lead to the increase of mitochondrial ROS, thus promoting ferroptosis and necrosis. Specifically, CHAC1 overexpression can increase ROS levels, induce mitochondrial dysfunction, and ultimately lead to cell death through ferroptosis and necrosis.[43–45]

However, there is a lack of relevant literature to support the relationship between PAPR9 and LCN2 and ferroptosis and necroptosis, suggesting that CHAC1 might be a more important research target.

Despite the strengths of this study, several limitations should be acknowledged. First, the retrospective and in silico study design inherently limits the ability to draw causal inferences and may introduce selection bias. Second, our analyses relied on bulk transcriptomic data, which can mask cellular heterogeneity and obscure disease-relevant signals from minority cell populations. Third, the methylation dataset included only a small sample size (3 psoriatic and 9 control samples), limiting the robustness and generalizability of our epigenetic findings. Fourth, clinical confounders such as treatment status could not be fully controlled due to restricted sample annotation, and may influence gene expression or methylation results. Finally, our study lacks experimental validation. Thus, the mechanistic roles of candidate molecules and their relevance in vivo remain to be confirmed.

The successful development of biomarkers in the clinic will provide a strong impetus for the development and production of the combination of CHAC1, PARP9, and LCN2 biomarkers as a psoriasis kit. The introduction of the CHAC1, PARP9, and LCN2 kits will provide patients with psoriasis with a new diagnostic pathway, but currently most patients prefer traditional diagnostic tools, such as imaging tests, rather not biomarker testing, which may be related to the fact that biomarker testing is not included in the universal health insurance. More importantly, biomarker testing can more accurately identify specific mutated genes in patients than traditional testing, which may provide a powerful guide for the diagnosis and treatment of the disease.[62]

At present, our study is confined to the examination of CHAC1 as a prospective biomarker for psoriasis, aiming to elucidate its role in regulating ferroptosis in activated CD4 T cells, neutrophils, Tregs, and Th2 cells within psoriasis development. In the future, it may be necessary to construct cell and animal models of psoriasis, clinical samples, and preclinical studies to further validate its clinical utility.

Conclusion

In this study, we screened for ferroptosis-related biomarkers CHAC1, PARP9, and LCN2 by multiple machine learning algorithms. For the first time, we revealed a group of psoriasis patients with more severe lesions by ferroptosis typing and analysed their immune profile in detail. CHAC1 regulates ferroptosis in activated CD4 T cells, neutrophils, Tregs and Th2 during psoriasis development and exacerbates psoriasis development.

Abbreviations

AUC, Area Under the Curve; DCA, Decision Curve Analysis; DEGs, Differentially Expressed Genes; GO, Gene Ontology; FRGs, Ferroptosis-Related Genes; GBDT, Gradient Boosting Decision Tree; GEO, Gene Expression Omnibus; KEGG, Kyoto Encyclopedia of Genes and Genomes; LASSO, Least Absolute Shrinkage and Selection Operator; ME, Module Eigengene; PCA, Principal Component Analysis; PPI, Protein-Protein Interaction.

Data Sharing Statement

Four RNA-seq datasets were obtained from Gene Expression Omnibus (GEO, https://www.ncbi.nlm.nih.gov/geo), GSE30999, GSE13355, GSE14905 and GSE103038. Ferroptosis-related genes were obtained from the FerrDb database (http://www.zhounan.org/ferrdb/).

Ethics Approval and Informed Consent

The datasets used in this research were directly obtained from the GEO public data platform (https://www.ncbi.nlm.nih.gov/geo/). GEO is a public database that encompasses patients who have obtained ethical approval. This research was approved by the Clinical Research Ethics Committee of Affiliated Hospital of Guangdong Medical University (YJKT2025-246-01).

Acknowledgments

We would like to thank Chen Xu, Li Min, Hospital of Dermatology, Chinese Academy of Medical Sciences for support.

Funding

The author(s) declare that financial support was received for the research, authorship, and/or publication of this article. The work was funded by (1) the High-level Talent Research Start-up Project of Affiliated Hospital of Guangdong Medical University (GCC2023027) and (2) Affiliated Hospital of Guangdong Medical University Clinical Research Program (LCYJ2021B009).

Disclosure

The authors declare no competing interests.

References

1. Parisi R, Iskandar IYK, Kontopantelis E, et al. National, regional, and worldwide epidemiology of psoriasis: systematic analysis and modelling study. *BMJ*. 2020;369:m1590. doi:10.1136/bmj.m1590
2. Kaushik SB, Lebwohl MG. Psoriasis: which therapy for which patient: psoriasis comorbidities and preferred systemic agents. *J Am Acad Dermatol*. 2019;80(1):27–40. doi:10.1016/j.jaad.2018.06.057
3. H H Chen, S R Abed. Update aetiopathogenesis and treatment of psoriasis: a literature review. *J Dermatol Res*. 2023;4. doi:10.46889/jdr.2023
4. Li J, Cao F, Yin H-L, et al. Ferroptosis: past, present and future. *Cell Death Dis*. 2020;11(2):88. doi:10.1038/s41419-020-2298-2
5. Qiu Y, Cao Y, Cao W, Jia Y, Lu N. The application of ferroptosis in diseases. *Pharmacol Res*. 2020;159:104919. doi:10.1016/j.phrs.2020.104919
6. Tsurusaki S, Tsuchiya Y, Koumura T, et al. Hepatic ferroptosis plays an important role as the trigger for initiating inflammation in nonalcoholic steatohepatitis. *Cell Death Dis*. 2019;10(6):449. doi:10.1038/s41419-019-1678-y
7. Chen B, Chen Z, Liu M, et al. Inhibition of neuronal ferroptosis in the acute phase of intracerebral hemorrhage shows long-term cerebroprotective effects. *Brain Res Bull*. 2019;153:122–132. doi:10.1016/j.brainresbull.2019.08.013
8. Kökçam I, Naziroğlu M. Antioxidants and lipid peroxidation status in the blood of patients with psoriasis. *Clin Chim Acta*. 1999;289(1–2):23–31. doi:10.1016/s0009-8981(99)00150-3
9. Mungrue IN, Pagnon J, Kohannim O, Gargalovic PS, Lusis AJ. CHAC1/MGC4504 is a novel proapoptotic component of the unfolded protein response, downstream of the ATF4-ATF3-CHOP cascade. *J Immunol*. 2009;182:466–476. doi:10.4049/jimmunol.182.1.466
10. Gagliardi M, Cotella D, Santoro C, et al. Aldo-keto reductases protect metastatic melanoma from ER stress-independent ferroptosis. *Cell Death Dis*. 2019;10(12):902. doi:10.1038/s41419-019-2143-7
11. Zhao J, Shen J, Mao L, et al. Cancer associated fibroblast secreted miR-432-5p targets CHAC1 to inhibit ferroptosis and promote acquired chemoresistance in prostate cancer. *Oncogene*. 2024;43(27):2104–2114. doi:10.1038/s41388-024-03057-6
12. Zhou L, Zhong Y, Li C, et al. MAPK14 as a key gene for regulating inflammatory response and macrophage M1 polarization induced by ferroptotic keratinocyte in psoriasis. *Inflammation*. 2024;47(5):1564–1584. doi:10.1007/s10753-024-01994-8
13. Xiao X, Yeoh BS, Vijay-Kumar M. Lipocalin 2: an emerging player in iron homeostasis and inflammation. *Annu Rev Nutr*. 2017;37(1):103–130. doi:10.1146/annurev-nutr-071816-064559

14. Zhan J, Chen J, Deng L, Lu Y, Luo L. Exploring the ferroptosis-related gene lipocalin 2 as a potential biomarker for sepsis-induced acute respiratory distress syndrome based on machine learning. *Biochim Biophys Acta Mol Basis Dis*. 2024;1870(4):167101. doi:10.1016/j.bbadis.2024.167101
15. Deng L, He S, Guo N, et al. Molecular mechanisms of ferroptosis and relevance to inflammation. *Inflamm Res*. 2023;72(2):281–299. doi:10.1007/s00011-022-01672-1
16. Shao S, Cao T, Jin L, et al. Increased lipocalin-2 contributes to the pathogenesis of psoriasis by modulating neutrophil chemotaxis and cytokine secretion. *J Invest Dermatol*. 2016;136(7):1418–1428. doi:10.1016/j.jid.2016.03.002
17. Ma J, Chen J, Xue K, et al. LCN2 mediates skin inflammation in psoriasis through the SREBP2–NLRC4 axis. *J Invest Dermatol*. 2022;142(8):2194–2204.e2111. doi:10.1016/j.jid.2022.01.012
18. Seiringer P, Hillig C, Schäbitz A, et al. Spatial transcriptomics reveals altered lipid metabolism and inflammation-related gene expression of sebaceous glands in psoriasis and atopic dermatitis. *Front Immunol*. 2024;15:1334844. doi:10.3389/fimmu.2024.1334844
19. Fujii K, Yamamoto Y, Mizutani Y, Saito K, Seishima M. Indoleamine 2,3-dioxygenase 2 deficiency exacerbates imiquimod-induced psoriasis-like skin inflammation. *Int J Mol Sci*. 2020;21(15):5515. doi:10.3390/ijms21155515
20. El-Rifaie AA, Sabry D, Doss RW, Kamal MA, Abd El Hassib DM. Heme oxygenase and iron status in exosomes of psoriasis patients. *Arch Dermatol Res*. 2018;310(8):651–656. doi:10.1007/s00403-018-1852-6
21. Li Y, Lin P, Wang S, et al. Quantitative analysis of differentially expressed proteins in psoriasis vulgaris using tandem mass tags and parallel reaction monitoring. *Clin Proteomics*. 2020;17(1):30. doi:10.1186/s12014-020-09293-8
22. Abdou AG, Farag AGA, Abdelaziz RA, et al. Immunolocalization of MUC1 in chronic plaque psoriasis. *J Immunoassay Immunochem*. 2019;40(5):515–527. doi:10.1080/15321819.2019.1646660
23. Koczan D, Guthke R, Thiesen H-J, et al. Gene expression profiling of peripheral blood mononuclear leukocytes from psoriasis patients identifies new immune regulatory molecules. *Eur J Dermatol*. 2005;15(4):251–257.
24. Greb JE, Goldminz AM, Elder JT, et al. Psoriasis. *Nat Rev Dis Primers*. 2016;2(1):16082. doi:10.1038/nrdp.2016.82
25. Egeberg A, Thyssen JP, Wu JJ, Skov L. Risk of first-time and recurrent depression in patients with psoriasis: a population-based cohort study. *Br J Dermatol*. 2019;180(1):116–121. doi:10.1111/bjd.17208
26. Parisi R, Symmons DP, Griffiths CE, Ashcroft DM. Global epidemiology of psoriasis: a systematic review of incidence and prevalence. *J Invest Dermatol*. 2013;133(2):377–385. doi:10.1038/jid.2012.339
27. Di Meglio P, Villanova F, Nestle FO. Cold spring harb perspect med. *Cold Spring Harbor Perspectives in Medicine*. 2014;4(8). doi:10.1101/cshperspect.a015354
28. Bai Y, Meng L, Han L, et al. Lipid storage and lipophagy regulates ferroptosis. *Biochem Biophys Res Commun*. 2019;508(4):997–1003. doi:10.1016/j.bbrc.2018.12.039
29. Jiang X, Stockwell BR, Conrad M. Ferroptosis: mechanisms, biology and role in disease. *Nat Rev Mol Cell Biol*. 2021;22(4):266–282. doi:10.1038/s41580-020-00324-8
30. Li S, Luo X, Zhang S, et al. Ferroptosis activation contributes to the formation of skin lesions in psoriasis vulgaris. *Antioxidants*. 2023;12. doi:10.3390/antiox12020310
31. Yang WS, SriRamaratnam R, Welsch M, et al. Regulation of ferroptotic cancer cell death by GPX4. *Cell*. 2014;156(1–2):317–331. doi:10.1016/j.cell.2013.12.010
32. Sun Y, Chen P, Zhai B, et al. The emerging role of ferroptosis in inflammation. *Biomed Pharmacother*. 2020;127:110108. doi:10.1016/j.biopha.2020.110108
33. Zhou Q, Yang L, Li T, et al. Mechanisms and inhibitors of ferroptosis in psoriasis. *Front Mol Biosci*. 2022;9(1019447). doi:10.3389/fmolb.2022.1019447
34. Laporte M, Galand P, Fokan D, de Graef C, Heenen M. Apoptosis in established and healing psoriasis. *Dermatology*. 2000;200(4):314–316. doi:10.1159/000018394
35. Lachner J, Mlitz V, Tschachler E, Eckhart L. Epidermal cornification is preceded by the expression of a keratinocyte-specific set of pyroptosis-related genes. *Sci Rep*. 2017;7(1):17446. doi:10.1038/s41598-017-17782-4
36. Zhang JY, Zhou B, Sun R-Y, et al. The metabolite α-KG induces GSDMC-dependent pyroptosis through death receptor 6-activated caspase-8. *Cell Res*. 2021;31(9):980–997. doi:10.1038/s41422-021-00506-9
37. Kaur M, Bahia MS, Silakari O. Inhibitors of interleukin-2 inducible T-cell kinase as potential therapeutic candidates for the treatment of various inflammatory disease conditions. *Eur J Pharm Sci*. 2012;47(3):574–588. doi:10.1016/j.ejps.2012.07.013
38. Chugh P, Paluch EK. The actin cortex at a glance. *J Cell Sci*. 2018;131(14). doi:10.1242/jcs.186254
39. Salbreux G, Charras G, Paluch E. Actin cortex mechanics and cellular morphogenesis. *Trends Cell Biol*. 2012;22(10):536–545. doi:10.1016/j.tcb.2012.07.001
40. Sun LD, Cheng H, Wang Z-X, et al. Association analyses identify six new psoriasis susceptibility loci in the Chinese population. *Nat Genet*. 2010;42(11):1005–1009. doi:10.1038/ng.690
41. Cheng JB, Sedgewick AJ, Finnegan AI, et al. Transcriptional programming of normal and inflamed human epidermis at single-cell resolution. *Cell Rep*. 2018;25(4):871–883. doi:10.1016/j.celrep.2018.09.006
42. Grundy SM. Metabolic syndrome update. *Trends Cardiovasc Med*. 2016;26(4):364–373. doi:10.1016/j.tcm.2015.10.004
43. Sun J, Ren H, Wang J, et al. CHAC1: a master regulator of oxidative stress and ferroptosis in human diseases and cancers. *Front Cell Dev Biol*. 2024;12:1458716. doi:10.3389/fcell.2024.1458716
44. Szántó M, Gupte R, Kraus WL, Pacher P, Bai P. PARPs in lipid metabolism and related diseases. *Prog Lipid Res*. 2021;84:101117. doi:10.1016/j.plipres.2021.101117
45. Ren K, Peng X, Duan X, et al. Synergistic effects of LCN2 and TWEAK on the progression of psoriasis. *Cell Mol Immunol*. 2025;22(7):760–775. doi:10.1038/s41423-025-01292-9
46. Yuyun X, Fan Y, Weiping W, Qing Y, Bingwei S. Metabolomic analysis of spontaneous neutrophil apoptosis reveals the potential involvement of glutathione depletion. *Innate Immun*. 2021;27(1):31–40. doi:10.1177/1753425920951985
47. Griffiths CE, Voorhees JJ. T cells and autoimmunity. *J R Soc Med*. 1996;89(6):315–319. doi:10.1177/014107689608900604

48. Lowes MA, Kikuchi T, Fuentes-Duculan J, et al. Psoriasis vulgaris lesions contain discrete populations of Th1 and Th17 T cells. *J Invest Dermatol*. 2008;128(5):1207–1211. doi:10.1038/sj.jid.5701213
49. Nikaein A, Phillips C, Gilbert SC, et al. Characterization of skin-infiltrating lymphocytes in patients with psoriasis. *J Invest Dermatol*. 1991;96(1):3–9. doi:10.1111/1523-1747.ep12514646
50. Perera GK, Di Meglio P, Nestle FO. Psoriasis. *Annu Rev Pathol*. 2012;7(1):385–422. doi:10.1146/annurev-pathol-011811-132448
51. Belizário JE, Brandão W, Rossato C, Peron JP. Thymic and postthymic regulation of naïve CD4(+) T-cell lineage fates in humans and mice models. *Mediators Inflamm*. 2016;2016:9523628. doi:10.1155/2016/9523628
52. Mrowietz U. Neutrophils' sexiness is independent of trendy fashion. *Exp Dermatol*. 2017;26:312–313. doi:10.1111/exd.13102
53. Polat M, Bugdayci G, Kaya H, Oğuzman H. Evaluation of neutrophil-to-lymphocyte ratio and platelet-to-lymphocyte ratio in Turkish patients with chronic plaque psoriasis. *Acta Dermatovenerol Alp Pannonica Adriat*. 2017;26:97–100. doi:10.15570/actaapa.2017.28
54. Paliogiannis P, Satta R, Deligia G, et al. Associations between the neutrophil-to-lymphocyte and the platelet-to-lymphocyte ratios and the presence and severity of psoriasis: a systematic review and meta-analysis. *Clin Exp Med*. 2019;19(1):37–45. doi:10.1007/s10238-018-0538-x
55. Balevi A, Olmuşçelik O, Ustuner P, Özdemir M. Is there any correlation between red cell distribution width, mean platelet volume neutrophil count, lymphocyte count, and psoriasis area severity index in patients under treatment for psoriasis? *Acta Dermatovenerol Croat*. 2018;26:199–205.
56. Schön MP, Broekaert SM, Erpenbeck L. Sexy again: the renaissance of neutrophils in psoriasis. *Exp Dermatol*. 2017;26:305–311. doi:10.1111/exd.13067
57. Sugiyama H, Gyulai R, Toichi E, et al. Dysfunctional blood and target tissue CD4+CD25high regulatory T cells in psoriasis: mechanism underlying unrestrained pathogenic effector T cell proliferation. *J Immunol*. 2005;174(1):164–173. doi:10.4049/jimmunol.174.1.164
58. Zhang K, Li X, Yin G, et al. Functional characterization of CD4+CD25+ regulatory T cells differentiated in vitro from bone marrow-derived haematopoietic cells of psoriasis patients with a family history of the disorder. *Br J Dermatol*. 2008;158(2):298–305. doi:10.1111/j.1365-2133.2007.08359.x
59. Zhang L, Yang XQ, Cheng J, Hui RS, Gao TW. Increased Th17 cells are accompanied by FoxP3(+) Treg cell accumulation and correlated with psoriasis disease severity. *Clin Immunol*. 2010;135(1):108–117. doi:10.1016/j.clim.2009.11.008
60. Zhang L, Li Y, Yang X, et al. Characterization of Th17 and FoxP3 + Treg cells in paediatric psoriasis patients. *Scand J Immunol*. 2016;83(3):174–180. doi:10.1111/sji.12404
61. Basit F, van Oppen LM, Schöckel L, et al. Mitochondrial complex I inhibition triggers a mitophagy-dependent ROS increase leading to necroptosis and ferroptosis in melanoma cells. *Cell Death Dis*. 2017;8(3):e2716. doi:10.1038/cddis.2017.133
62. Kim H, Kwon HJ, Kim ES, et al. Comparison of the predictive power of a combination versus individual biomarker testing in non-small cell lung cancer patients treated with immune checkpoint inhibitors. *Cancer Res Treat*. 2022;54(2):424–433. doi:10.4143/crt.2021.583